

## Influence of neighboring bubbles on the primary Bjerknes force acting on a small cavitation bubble in a strong acoustic field

Alexander A. Doinikov

*Institute of Nuclear Problems, Byelorussian State University, 11 Bobruiskaya Street, Minsk 220050, Belarus*

(Received 11 May 2000)

The primary Bjerknes force on a small bubble in a strong acoustic field in the presence of another bubble is calculated. It is shown that the influence of the bubbles on each other's primary Bjerknes forces is very substantial even if the separation distance between them is large compared with their size. As a result, the peculiarities of the primary forces in strong fields, such as the change of sign with increasing driving pressure amplitude, manifest themselves earlier and more vigorously. The results obtained are of immediate interest for understanding and modeling collective bubble phenomena in strong fields.

PACS number(s): 47.55.Bx, 47.55.Dz, 47.55.Kf, 43.25.+y

This study was inspired by papers [1] and [2], which examine the time-averaged radiation forces experienced by small gas bubbles in a strong acoustic field. The first paper deals with the force on a single bubble, called the *primary Bjerknes force*, and the second with the interaction force between two bubbles, known as the *secondary Bjerknes force*. Both papers are of immediate consequence for understanding and modeling collective bubble phenomena in high-pressure fields, such as multibubble sonoluminescence and acoustic streamer formation. They were motivated by the fact that the classical Bjerknes theory does not apply under such conditions since it only allows for linear bubble oscillations.

The Bjerknes force (both primary and secondary) can be written as

$$\mathbf{F} = -\langle V \nabla p \rangle, \quad (1)$$

where  $V$  is the time-varying volume of the bubble involved,  $p$  is the incident pressure, and  $\langle \rangle$  denotes the time average over the period of the acoustic field. For a single bubble,  $p$  is the pressure of the external forcing,  $p_{ex}$ . Substituting it into Eq. (1),

$$\mathbf{F}_{pB1} = -\langle V \nabla p_{ex} \rangle, \quad (2)$$

and calculating the volume  $V(t)$  of the bubble using the Keller-Miksis model [3], one obtains the primary Bjerknes force allowing for nonlinear bubble oscillations. It is this approach that is used in [1]. In the case of two bubbles, setting in Eq. (1)  $V = V_1$  and  $p = p_2$ , where  $V_1$  is the time-varying volume of the first bubble and  $p_2$  is the scattered pressure of the second bubble, one obtains the secondary Bjerknes force acting from the second bubble on the first one as

$$\mathbf{F}_{sB1} = -\langle V_1 \nabla p_2 \rangle. \quad (3)$$

To take into account the radiation coupling between the bubbles, i.e., the influence of the bubbles' scattered fields on each other's pulsations, the Keller-Miksis equations for both bubbles are supplemented with corresponding terms (see below). This is what is done in [2] when investigating the effect of a strong field on the secondary Bjerknes force. But because of the presence of the second bubble not only does the pressure incident on the first bubble become equal to

$$p = p_{ex} + p_2 \quad (4)$$

but also the volume of the first bubble can be represented as

$$V_1 = V_{1ex} \oplus V_{12}, \quad (5)$$

where  $V_{1ex}$  is induced by  $p_{ex}$  and  $V_{12}$  by  $p_2$ . Of course, the plus here by no means denotes a linear superposition because the bubbles oscillate nonlinearly and hence the component  $V_{12}$  cannot be separated from  $V_{1ex}$ . To emphasize this, the plus is encircled. The presence of  $V_{12}$  means that, in addition to the forces given by Eqs. (2) and (3), there exists one more term, which can conventionally be written as

$$\mathbf{F}_{pB12} = -\langle V_{12} \nabla p_{ex} \rangle. \quad (6)$$

We say ‘‘conventionally’’ because in a strong field, as is mentioned above, the component (6) cannot be extracted from the total primary force. In a weak field, this is possible and calculation of the secondary Bjerknes force, which allows for the compressibility of the host fluid [4], does discover such a component directed along the gradient of the imposed field, which can be considered as an additional component of the secondary force since it depends on the spacing between the bubbles and vanishes when the spacing tends to infinity. In a strong field, however, it would be more correct to talk just about the influence of the second bubble on the primary force experienced by the first bubble. It is the purpose of the present paper to investigate this effect which went unnoticed in [1] and [2].

Let two gas bubbles with mean radii  $R_{10}$  and  $R_{20}$  and a distance  $L$  between their equilibrium centers be in a liquid exposed to an acoustic wave field. As an example, let us take a plane standing wave

$$p_{ex}(\mathbf{r}, t) = -P_a \sin \omega t \cos(\mathbf{k} \cdot \mathbf{r}), \quad (7)$$

where  $\omega$  is the angular frequency,  $\mathbf{k}$  is the wave vector, and  $\mathbf{r}$  is the position vector. Suppose that the wavelength of sound is much larger than  $L$  and that  $L \gg R_{10}, R_{20}$ . Then, when calculating the scattered fields of the bubbles, we can neglect both the compressibility of the host liquid and the shape deviations of the bubbles from sphericity. Under these conditions, the equations of the radial oscillations of the bubbles are given by [2]

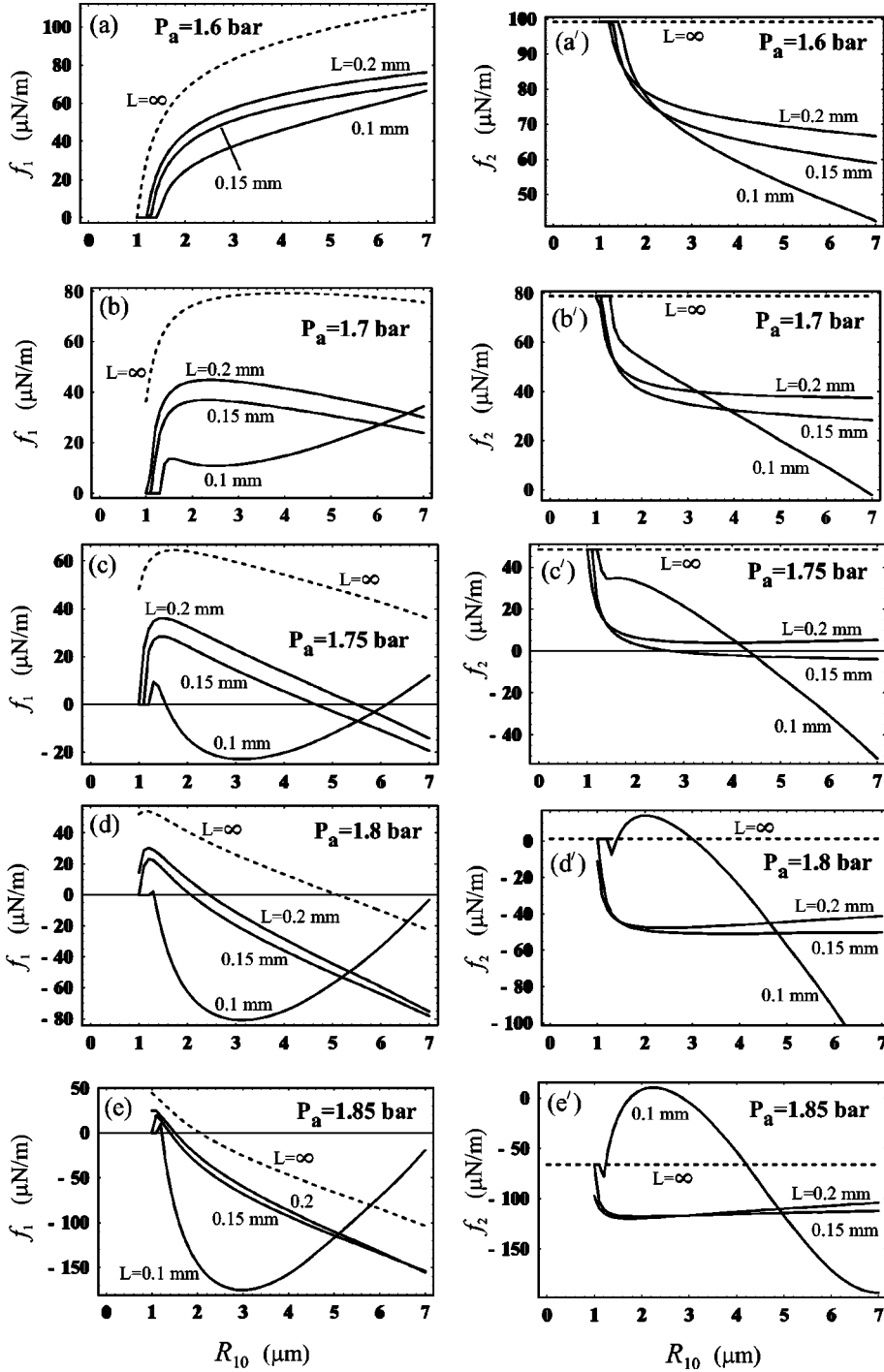


FIG. 1. The “stiffness coefficients”  $f_1$  (left column) and  $f_2$  (right column) vs  $R_{10}$  for different values of  $L$  and  $P_a$ . The dashed curves correspond to uncoupled bubbles ( $L \rightarrow \infty$ ).

$$\left(1 - \frac{\dot{R}_1}{c}\right) R_1 \ddot{R}_1 + \left(\frac{3}{2} - \frac{\dot{R}_1}{2c}\right) \dot{R}_1^2 = \frac{1}{\rho} \left(1 + \frac{\dot{R}_1}{c}\right) p_{s1} + \frac{R_1}{\rho c} \frac{dp_{s1}}{dt} - \frac{1}{L} \frac{d}{dt} (\dot{R}_2 R_2^2), \quad (8)$$

$$\left(1 - \frac{\dot{R}_2}{c}\right) R_2 \ddot{R}_2 + \left(\frac{3}{2} - \frac{\dot{R}_2}{2c}\right) \dot{R}_2^2 = \frac{1}{\rho} \left(1 + \frac{\dot{R}_2}{c}\right) p_{s2} + \frac{R_2}{\rho c} \frac{dp_{s2}}{dt} - \frac{1}{L} \frac{d}{dt} (\dot{R}_1 R_1^2), \quad (9)$$

where

$$p_{sj} = \left(P_0 + \frac{2\sigma}{R_{j0}}\right) \left(\frac{R_{j0}}{R_j}\right)^{3\gamma} - \frac{2\sigma}{R_j} - \frac{4\mu\dot{R}_j}{R_j} - P_0 - p_{ex}, \quad j=1,2, \quad (10)$$

$R_j(t)$  is the instantaneous radius of the  $j$ th bubble, the overdot denotes the time derivative,  $c$  is the speed of sound in the liquid,  $\rho$  is the density of the liquid,  $P_0$  is the hydrostatic pressure,  $\sigma$  is the surface tension,  $\gamma$  is the polytropic exponent of the gas, and  $\mu$  is the viscosity of the liquid. The last terms on the right-hand sides of Eqs. (8) and (9) describe the radiation coupling between the bubbles that is mentioned above. It is these terms that lead to the modification of the primary Bjerknes forces on the bubbles.

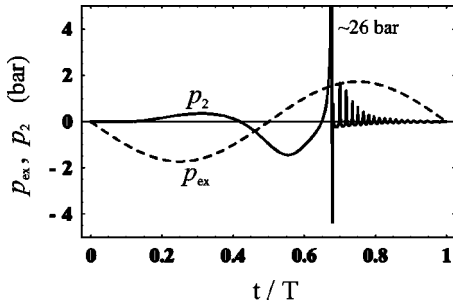


FIG. 2. The external sound pressure and the scattered pressure of the second bubble at the location of the first bubble during one driving period  $T=1/f$  for  $P_a=1.75$  bar,  $R_{10}=2 \mu\text{m}$ ,  $R_{20}=5 \mu\text{m}$ ,  $d_1=d_2=2$  mm, and  $L=0.1$  mm.

Substituting Eq. (7) into Eq. (2) and denoting the distance between the  $j$ th bubble and the nearest plane of pressure antinodes by  $d_j$ , one obtains the primary force on the bubble as

$$\mathbf{F}_j = -\frac{4}{3} \pi P_a \mathbf{k} \sin kd_j \langle R_j^3(t) \sin \omega t \rangle. \quad (11)$$

If the bubbles are in the close vicinity of the pressure antinode so that  $kd_j \ll 1$ , Eq. (11) may be rewritten in the following way:

$$\mathbf{F}_j = -f_j \mathbf{d}_j, \quad f_j = \frac{4}{3} \pi k^2 P_a \langle R_j^3(t) \sin \omega t \rangle, \quad (12)$$

where the vector  $\mathbf{d}_j$ , with length  $d_j$ , is directed from the pressure antinode to the  $j$ th bubble. Equation (12) shows that in the vicinity of pressure antinodes the primary Bjerknes force behaves like a spring with effective stiffness  $f_j$ , which can change its sign. If  $f_j > 0$ , then bubbles are attracted to the pressure antinodes. If  $f_j < 0$ , then bubbles are repelled. Recall that in a weak field bubbles driven below their linear resonance frequencies move toward pressure antinodes, while bubbles driven above linear resonance undergo a repulsive force [5]. It was shown in [1] that in high-pressure fields this is not always the case. If the forcing is strong enough, small bubbles, i.e., those driven well below linear resonance, can be repelled from pressure antinodes. It will be shown here that the influence of neighboring bubbles can substantially precipitate the changeover of the primary force.

Numerical calculations have been made for the same physical parameters as in [1] and [2], namely, assuming that the host liquid is water, the gas within the two bubbles is air, the driving frequency  $f=20$  kHz, the driving pressure amplitude  $P_a > 1$  bar, and the equilibrium bubble radii are on the order of a few micrometers. The bubble radii  $R_1(t)$  and  $R_2(t)$  were computed from Eqs. (8) and (9) using the program MATHEMATICA and then utilized in calculating the “stiffness coefficients”  $f_1$  and  $f_2$  by Eq. (12). The results obtained are shown in Fig. 1. The left column, Figs. 1(a)–1(e), displays  $f_1$  versus  $R_{10}$  for different values of the separation distance  $L$  and the driving pressure amplitude  $P_a$ . It is assumed that  $R_{20}=5 \mu\text{m}$  and that the bubbles are at equal distances from the pressure antinode,  $d_1=d_2=2$  mm. The right column, Figs. 1(a')–1(e'), shows the behavior of  $f_2$ . The dashed curves give  $f_1$  and  $f_2$  for uncoupled bubbles, i.e., for  $L \rightarrow \infty$ . It is seen that with increasing driving pressure amplitude  $P_a$  and decreasing separation distance  $L$  the influ-

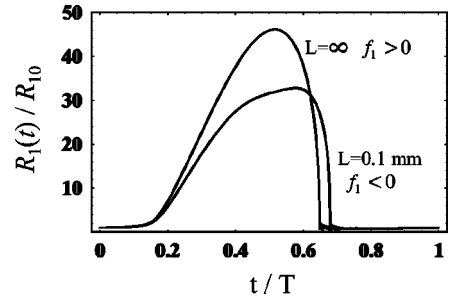


FIG. 3. The oscillations of the first bubble during one driving period in the absence ( $L=\infty$ ) and in the presence ( $L=0.1$  mm) of the second bubble. Parameters are as in Fig. 2.

ence of the bubbles on each other’s primary forces becomes progressively stronger. For smaller  $P_a$ , Fig. 1(a), the presence of the second bubble tangibly slows down the growth of  $f_1$ . For higher  $P_a$ , Figs. 1(b)–1(e), the nonmonotonic dependence of  $f_1$  on  $R_{10}$ , which was first noted in [1], becomes very much more pronounced. In particular, the change of the force from attraction to repulsion occurs at much smaller values of  $R_{10}$ . The  $L=0.1$  mm curve in Fig. 1(c) even changes its sign twice, indicating that for  $R_{10} > R_{20}$  the primary force again becomes attractive. The primary Bjerknes force on the second bubble, whose equilibrium radius is here kept constant, is also subject to a strong modification. As  $R_{10}$  is increased, the primary force on the second bubble decreases; the smaller  $L$ , the smaller values  $f_2$  arrives at [see Figs. 1(a') and 1(b')]. For higher  $P_a$ , the force becomes repulsive just like that on the first bubble. Figure 1(d') also shows that the force can change its sign three times as  $R_{10}$  is increased, becoming consecutively repulsive, attractive, and repulsive again. This changeable behavior is likely to be accounted for by complex processes that accompany the first bubble passing through nonlinear resonance (dynamical Blake threshold) [1,2].

Figures 2 and 3 help in understanding why the influence of the second bubble is so large. Figure 2 shows the driving pressure  $p_{ex}$  and the scattered pressure of the second bubble  $p_2$  at the center of the first bubble under the conditions corresponding to the point  $R_{10}=2 \mu\text{m}$  of the lowermost curve in Fig. 1(c). It is seen that the contribution of the second bubble is comparable to and out of phase with the driving field. This leads to what is observed in Fig. 3, where the oscillations of the first bubble with and without the second bubble are plotted. It is known that the magnitude and sign of the primary Bjerknes force depend on the magnitude of the bubble response and the phase of the bubble collapse relative to the phase of the driving pressure [1]. It is seen from Fig. 3 that the additional pressure field generated by the second bubble depresses the response of the first bubble and changes its phase, moving the instant of the collapse deeper into the compression part of the driving pressure. As a result, the force on the first bubble becomes repulsive earlier (for a lower driving pressure amplitude) than in the case of a single bubble.

The results presented show that neighboring bubbles very substantially affect each other’s primary Bjerknes forces even if separation distances between them are large compared with their size. The effect is built up with increasing acoustic pressure amplitude. As a result, the peculiar features

of the primary Bjerknes forces in strong fields, such as the changeover from attraction to repulsion, manifest themselves much earlier and more violently. This suggests that adequate modeling of collective bubble phenomena in strong fields is

impossible unless mutual interactions between bubbles are properly accounted for.

This research was supported by the European Commission under the INCO Copernicus program.

---

[1] I. Akhatov, R. Mettin, C.D. Ohl, U. Parlitz, and W. Lauterborn, *Phys. Rev. E* **55**, 3747 (1997).

[2] R. Mettin, I. Akhatov, U. Parlitz, C.D. Ohl, and W. Lauterborn, *Phys. Rev. E* **56**, 2924 (1997).

[3] J.B. Keller and M. Miksis, *J. Acoust. Soc. Am.* **68**, 628 (1980).

[4] A.A. Doinikov and S.T. Zavtrak, *J. Acoust. Soc. Am.* **102**, 1424 (1997).

[5] A.I. Eller, *J. Acoust. Soc. Am.* **43**, 170 (1968).